environmental microbiology

Environmental Microbiology (2022) **00**(00), 00–00 doi:10.1111/1462-2920.15997

Strong seasonal differences of bacterial polysaccharide utilization in the North Sea over an annual cycle

Greta Giljan,[1] **Carol Arnosti**,[2] **Inga V. Kirstein**,[3] **Rudolf Amann**[1] **and Bernhard M. Fuchs**[1*]

[1]*Department of Molecular Ecology, Max Planck Institute for Marine Microbiology, Bremen, Germany.*

[2]*Department of Marine Sciences, University of North Carolina-Chapel Hill, Chapel Hill, NC.*

[3]*Alfred-Wegner-Institute Helmholtz-Center for Polar and Marine Research, Biological Station Helgoland, Helgoland, Germany.*

Summary

Marine heterotrophic bacteria contribute considerably to global carbon cycling, in part by utilizing phytoplankton-derived polysaccharides. The patterns and rates of two different polysaccharide utilization modes – extracellular hydrolysis and selfish uptake – have previously been found to change during spring phytoplankton bloom events. Here we investigated seasonal changes in bacterial utilization of three polysaccharides, laminarin, xylan and chondroitin sulfate. Strong seasonal differences were apparent in mode and speed of polysaccharide utilization, as well as in bacterial community compositions. Compared to the winter month of February, during the spring bloom in May, polysaccharide utilization was detected earlier in the incubations and a higher portion of all bacteria took up laminarin selfishly. Highest polysaccharide utilization was measured in June and September, mediated by bacterial communities that were significantly different from spring assemblages. Extensive selfish laminarin uptake, for example, was detectible within a few hours in June, while extracellular hydrolysis of chondroitin was dominant in September. In addition to the well-known *Bacteroidota* and *Gammaproteobacteria* clades, the numerically minor verrucomicrobial clade *Pedosphaeraceae* could be identified as a rapid laminarin utilizer. In summary, polysaccharide utilization proved highly variable over the seasons, both in mode and speed, and also by the bacterial clades involved.

Received 8 November, 2021; revised 26 March, 2022; accepted 2 April, 2022. *For correspondence. E-mail bfuchs@mpi-bremen.de; Tel. +49 421 2028 9350.

Introduction

Heterotrophic bacterial communities recycle about half of the carbon fixed by marine phytoplankton in the oceans (Azam *et al*., 1983). A major portion of phytoplankton biomass consists of structural and storage polysaccharides (e.g. Biersmith and Benner, 1998; Lee *et al*., 2004); heterotrophic bacteria are well-suited to degrade phytoplankton-derived polysaccharides, especially in temperate environments (Teeling *et al*., 2012; Moran *et al*., 2016; Teeling *et al*., 2016). In particular, many bacteria have a considerable complement of specialized enzymes (e.g. Helbert, 2017) that are suited to degrade complex polysaccharides that vary in monomer composition, structural linkage types and chemical side-groups (Laine, 1994; McCarthy *et al*., 1996; Aluwihare and Repeta, 1999). Two fundamentally different modes of polysaccharide utilization are currently known to be used by heterotrophic bacteria. One is the extracellular hydrolysis of polysaccharides to oligo- and monomeric compounds through hydrolytic enzymes attached to the outer membrane or freely released into the environment. Hydrolysis products are either taken up by the cell itself or serve as a source of substrates accessible for other 'scavenging' bacteria (Dunny *et al*., 2008; Reintjes *et al*., 2019). A second mode is the direct, selfish uptake mechanism, recently demonstrated by Cuskin *et al*. (2015) for gut bacteria, which includes the binding of the polysaccharide at the cell surface, partial hydrolysis to smaller poly- or oligosaccharide fragments, and subsequent uptake into the periplasm of the cell without loss of hydrolysis products to the external environment.

Extracellular hydrolysis of a range of different fluorescently labelled polysaccharides (FLA-PS) has been shown to occur in pelagic (e.g. Arnosti, 2008; Cardman *et al*., 2014; Hoarfrost *et al*., 2019) as well as benthic (e.g. Arnosti, 1995; Arnosti, 1996; Arnosti and Jørgensen, 2006; Arnosti, 2008) marine environments. Hydrolysis rates vary by substrate and location across different oceanic regions (e.g. Arnosti *et al*., 2011; Reintjes *et al*., 2019; Reintjes *et al*., 2020b) and at

different water depths (e.g. Balmonte *et al*., 2018; Reintjes *et al*., 2020b). Recently, serendipitous observations of fluorescently stained cells in incubations with FLA-PS demonstrated that the selfish mechanism plays an important role in ocean surface waters (Reintjes *et al*., 2017, 2019, 2020a & 2020b) and even in the deep ocean (Giljan *et al*., 2021). Either or both of these mechanisms could be used by the heterotrophic community to degrade a given polysaccharide, but the extent to which one is used can vary greatly (e.g. Reintjes *et al*., 2020a). The extent to which each mechanism is used also has implications for the availability of carbon substrates to the community, since they directly affect the size distribution and quantity of dissolved carbohydrates (Arnosti *et al*., 2018). When polysaccharides are consumed via the selfish mechanism, little to no low-molecular-weight oligo- or monosaccharides are made available to the rest of the microbial community. External hydrolysis, in contrast, leads to a shift in size spectrum, with large polysaccharides hydrolyzed to lower molecular weight oligo- and monosaccharides, which can be consumed also by bacteria that might not be able to degrade high-molecular-weight substrates. Which of these mechanisms is ultimately used likely depends on the genetic repertoire of the microbial community present, substrate availability and substrate structural complexity (Reintjes *et al*., 2020a; Arnosti *et al*., 2021).

To date, the dynamic interplay of these mechanisms over time has been studied only once, over the course of a spring bloom in Helgoland (Reintjes *et al*., 2020a). The early spring bloom was characterized by comparatively low selfish activity and low hydrolysis rates of only a few substrates. Both utilization mechanisms increased with progression of the bloom and increasing substrate availability, with selfish uptake increasing earlier and external hydrolysis peaking later in the late bloom phase. Only laminarin selfish uptake remained constantly high once the bloom commenced. Members of the *Bacteroidota*, the main responders to phytoplankton derived organic matter off Helgoland (Teeling *et al*., 2016; Kappelmann *et al*., 2019) were identified to use mainly laminarin and xylan through the selfish mechanism. In addition, *Gammaproteobacteria*, *Planctomycetota* (Boedeker *et al*., 2017; Reintjes *et al*., 2017; Reintjes *et al*., 2019) and *Verrucomicrobiota* (Martinez-Garcia *et al*., 2012; Cardman *et al*., 2014; Sichert *et al*., 2020) have been shown to behave selfishly, and other selfish bacteria remain to be identified.

In this study we examine bacterial polysaccharide utilization over a full annual cycle. To test whether the dynamic changes in selfish uptake and external hydrolysis observed over a spring phytoplankton bloom by Reintjes *et al*. (2020a) are representative of the dynamics during other seasons, we sampled five distinct time points: once before and once after the main phytoplankton peak during a spring bloom, once early and once late in a summer characterized by fluctuating phytoplankton abundances, and once in a winter situation after a long period of little phytoplankton presence. We measured selfish uptake of three different fluorescently labelled polysaccharides for each time point, and concurrently measured extracellular hydrolysis rates of the same substrates to investigate the use of each substrate processing mechanism. Laminarin, xylan and chondroitin sulfate were selected because they differ in molecular complexity, are present in large quantities in the ocean, and enzymes that hydrolyze these polysaccharides are widely distributed among marine bacteria (see Reintjes *et al*., 2017 and references therein). Bacterioplankton community composition was assessed by next-generation sequencing (NGS) of 16S rRNA, and was applied to identify potential bacterial groups using one or both polysaccharide utilization mechanisms at each time point. We additionally used fluorescence-activated cell sorting (FACS) to specifically sort FLA-PS stained cells and to determine their taxonomic affiliation.

Results

Changes in environmental parameters over the year

In 2018, water temperatures rose from 4°C in spring to more than 20°C in summer and declined again towards winter. Nitrate, phosphate and silicate concentrations followed the opposite trend (Fig. 1A, Supplementary Table S1) due to uptake by phytoplankton towards summer. Chlorophyll *a*, a proxy for phytoplankton abundance, increased to a peak of 7 $\mu g\, L^{-1}$ in late April. After this spring phytoplankton bloom, a few less pronounced peaks appeared in summer until the end of August, prior to a constant low (<1 $\mu g\, L^{-1}$) in winter. Specific phytoplankton groups varied in abundance, with centric diatoms (1.0×10^6 cells L^{-1}) dominating the spring bloom, and variably high abundances of coccolithophores and pennate diatoms, along with a high abundance of centric diatoms, throughout summer. Bacteria – the focused polysaccharide consumers of this study – followed the phytoplankton in quantity and tripled in abundance from spring to 2.3×10^9 cells L^{-1} in summer, dropping again below 1.0×10^9 cells L^{-1} in autumn (Fig. 1B).

Changes in bacterial polysaccharide utilization

Bacterial polysaccharide utilization was investigated at nine sampling dates in five strategically selected weeks from April 2018 to February 2019 at the long term ecological research (LTER) site Helgoland Roads. In four of the five sampling weeks, two biological replicates were

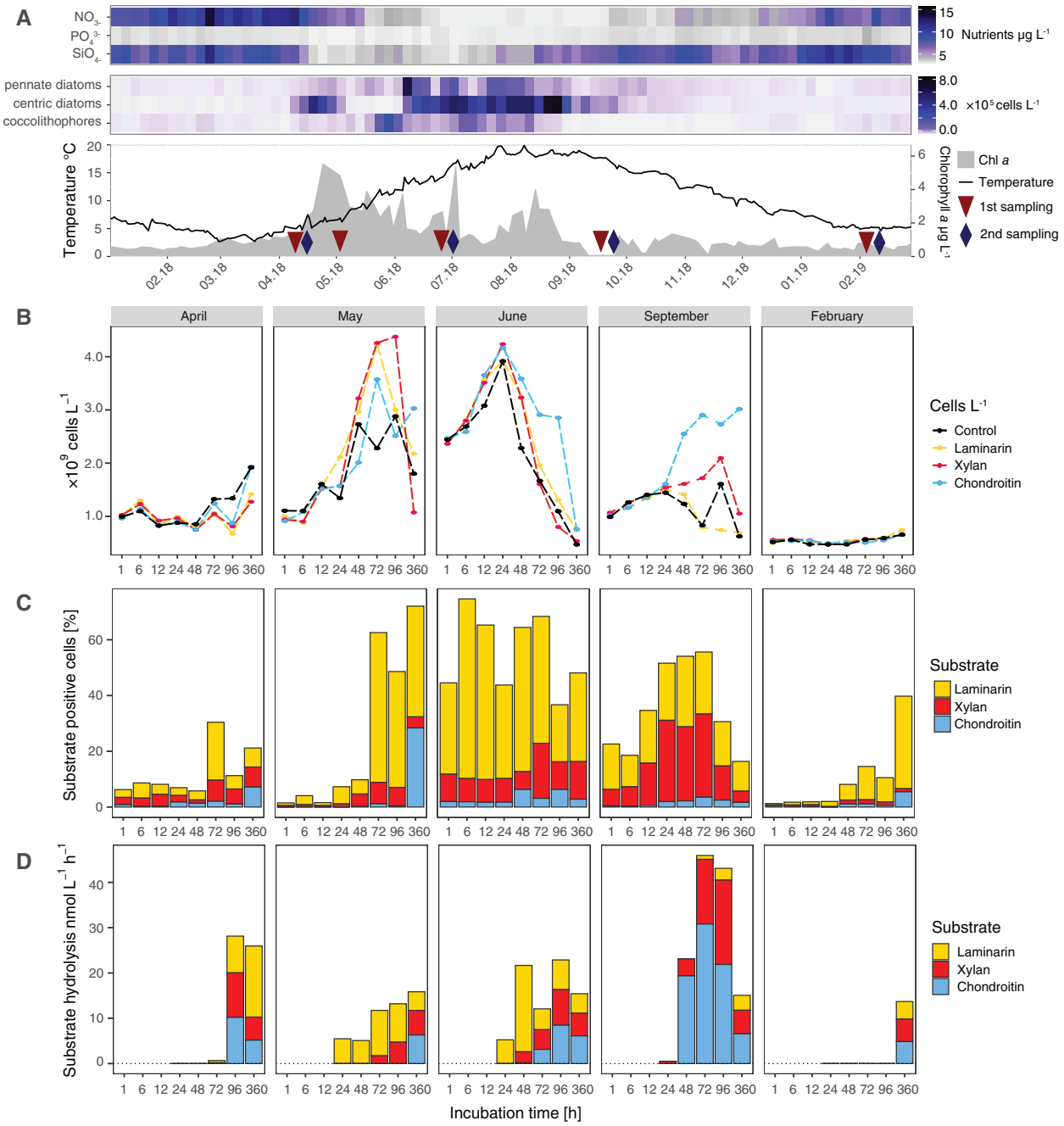

Fig. 1. Seasonal changes in heterotrophic polysaccharide utilization.
A. Changes in nutrient concentrations, phytoplankton abundance, water temperature and chlorophyll *a* (Chl *a*) concentration at the sampling site off Helgoland from February 2018 to February 2019. Arrowheads indicate the sampling time points in April (9th and 11th), May (5th), June (25th and 27th), September (17th and 19th) 2018 and February (5th and 7th) 2019.
B. Total cell counts over the course of the incubations with FLA-laminarin, FLA-xylan and FLA-chondroitin and the unamended treatment control. Bars of the amended incubations represent the average of six replicates ($n = 6$) and two (April, May) or six (June, September, February) of the unamended incubations.
C. Relative abundance of FLA-laminarin, FLA-xylan and FLA-chondroitin stained cells from the same flasks as in 1B ($n = 6$).
D. Extracellular hydrolysis rates of FLA-laminarin, FLA-xylan and FLA-chondroitin from the same flasks as in 1B ($n = 6$). Note that extracellular hydrolysis rate measurements were not conducted before 24 h of incubation time.

collected within 3 days. For each biological replicate, fluorescently labelled laminarin, xylan, or chondroitin sulfate was added individually to triplicate vials, and in addition, one unamended treatment control was incubated. Autoclaved seawater was used for killed control incubations (single incubations) for each polysaccharide.

Sample time points were more closely spaced (1, 5, 12, 24, 48 h) early in the incubation to characterize the *in situ* response of the bacterial community; later time points (72, 360 h) represent the overall potential of the bacterial community to utilize polysaccharides, allowing for induction of hydrolytic enzymes and cellular growth. From each incubation, the speed and extent of extracellular polysaccharide hydrolysis and selfish polysaccharide uptake were determined for the individual sampling time points (1, 6, 12, 24, 48, 72, 96 and 360 h); bacterial community composition and cell numbers were also measured from these same incubations. We define the 'speed' as period of time until polysaccharide utilization can be detected either by microscopic evidence of cellular selfish uptake or by measurement of extracellular hydrolysis: the shorter the period, the higher the 'speed'. The patterns in the type and speed of polysaccharides utilized proved to be reproducible among biological replicates, performed by similar bacterial communities on both days of sampling, as described below.

Bacterial cell numbers in amended and unamended incubations developed in parallel (Fig. 1B, Supplementary Figs S1A and B–S3A and B), but a seasonal dynamic was evident: the time point at which an increase in cell numbers was detected shifted to earlier times in the incubations from February to June. A peak in bacterial cells was detected in May and June after 72 and 24 h respectively. Only in September did cell abundance peak at 24 h for the laminarin amended and unamended incubations; cell counts increased further at later time points in September in the xylan and chondroitin sulfate amended incubations.

Selfish uptake of the FLA-polysaccharides laminarin, xylan and chondroitin was observed at all time points (Fig. 1C, Supplementary Figs S1C and D–S3C and D). In February, utilization of all three FLA-PS was low through both mechanisms, and extracellular hydrolysis could only be detected late in the incubation. Between February and May, the rate of extracellular hydrolysis, the speed of selfish uptake and the percentage of cells using the selfish mechanism increased for all three polysaccharides. This increase was least distinct for chondroitin sulfate, greater for xylan and most pronounced for laminarin. In particular, extracellular FLA-laminarin hydrolysis was first detected after 360 h in February, after 72 h in April, and in May was detected already after 24 h, then doubled to a peak of 10.0 nmol L^{-1} h^{-1} by the 72 h timepoint. In the same incubation, more than 50% of all cells were stained from selfish FLA-laminarin uptake. In June and September, substantial selfish uptake could be detected from the start of the incubations, accompanied by the highest extracellular hydrolysis rates as well as highest proportions of selfish bacteria of the entire year. In June, particularly the selfish uptake of laminarin stood out, with 30% of all cells stained within just 1 h of incubation, a proportion that increased to 60% after 6 h. Only in September did the proportions in utilization of the individual polysaccharides change: the highest percentage – 29% – of FLA-xylan-stained cells of all seasons was detected after 24 h, exceeding the proportion of FLA-laminarin stained cells in the September incubations. Additionally, extracellular xylan hydrolysis rates of 18.6 nmol L^{-1} h^{-1} and chondroitin hydrolysis rates of 30.8 nmol L^{-1} h^{-1} reached highest levels of the entire year, far exceeding laminarin hydrolysis rates.

Bacterial community composition

The ability to use specific polysaccharides is dependent on the initial bacterial community and the capabilities of its members. Monitoring changes in composition and abundance of bacterial communities during polysaccharide incubations aids in the identification of potential responders to specific conditions. For a robust statistical analysis of the communities, biological duplicates were sampled within 3 days in each sampling week (only one replicate for May), each of which was incubated in triplicate.

Non-metric multidimensional scaling (NMDS) analysis of 16S rRNA gene sequences demonstrated that the bacterial communities clustered by season. The added FLA-PS substrate did not influence clusters (Fig. 2A–C). At early incubation time points (0, 1 and 24 h), which are most representative of the initial communities, April and May communities were similar to each other; the communities in June and September also clustered together. April and May communities were mainly associated with increased Chl *a* concentrations, whereas the bacterial communities during June and September were more closely associated with high abundances of dinoflagellates, flagellates, diatoms, ciliates and coccolithophorids (Fig. 2D). In February, the community was distinctly different from all others, and correlated with high concentrations of silicate and phosphate. Upon extended incubation, a clear separation of the late incubation time points (72 and 360 h) from the initial community composition was observed in May, June and February (Fig. 2B). In April and September, there were only minor changes in community composition with incubation time.

Over the course of all incubations, changes in abundance and composition were observed among distinct members of the *Bacteroidota*, *Alphaproteobacteria* and *Gammaproteobacteria* (Fig. 3, Supplementary Figs S4–-S11). In April, the alphaproteobacterial clade SAR11 decreased, while *Gammaproteobacteria* (mainly 'Marine Methylotrophic Group 3' and *Colwellia*) and the bacteroidotal *Flavicella* increased in relative abundance over the incubation time. In May, again members of the

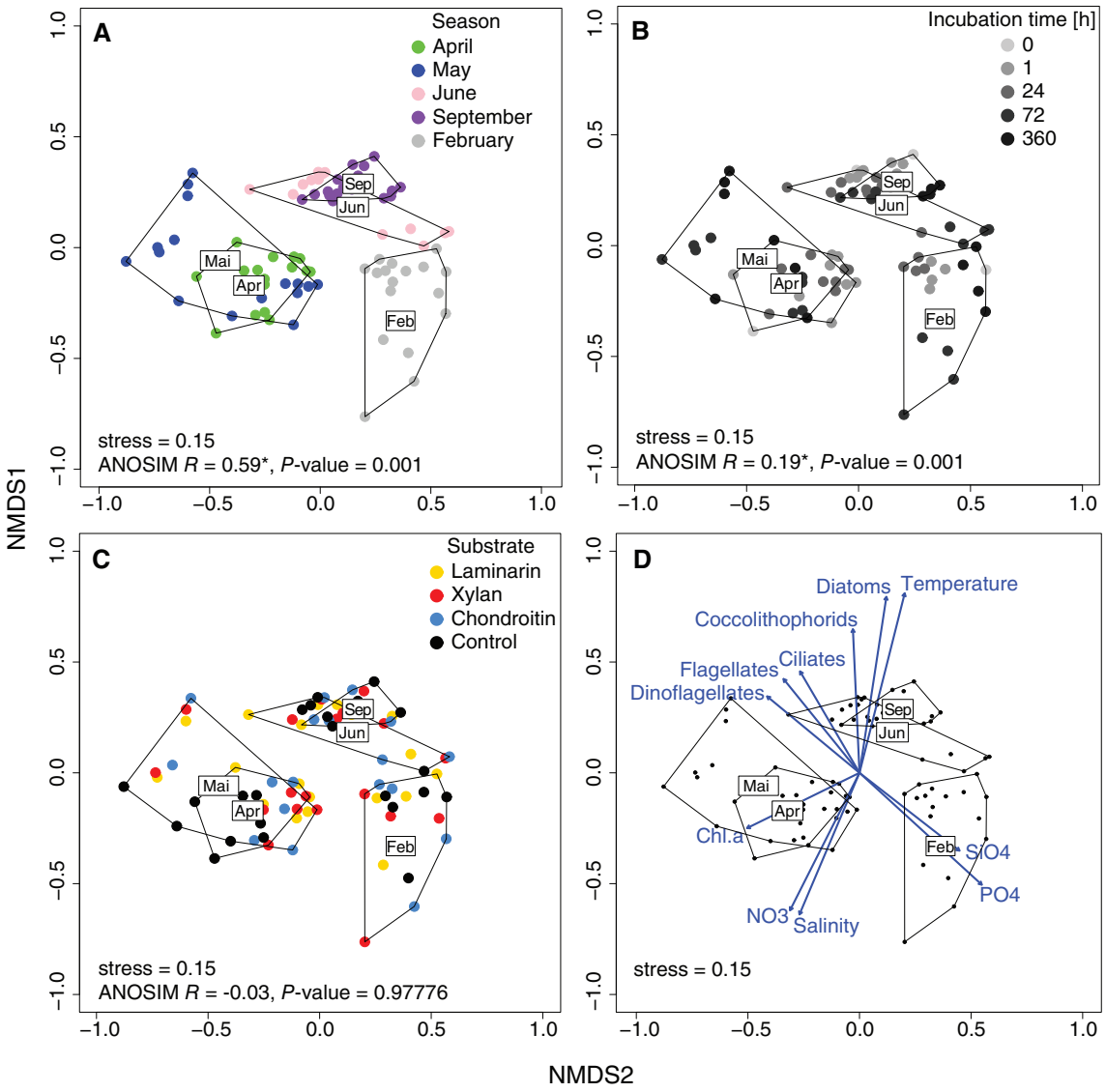

Fig. 2. Non-metric multidimensional scaling (NMDS) plot based on Bray–Curtis dissimilarity in bacterial communities. The community clusters by (A) time of sampling and (B) incubation time within the week of sampling but (C) not by supplemented polysaccharide. It was confirmed by statistical ANOSIM performed with 99 permutations on the community composition. Asterisk denotes statistical significant results. (D) Blue lines explain the influence of the respective environmental parameter on the NMDS ordination.

SAR11 clade decreased most in abundance, while the abundance of several *Gammaproteobacteria* and the bacteroidotal genus *Ulvibacter* (now *Ca*. Prosiliicoccus; Francis *et al*., 2019) increased in all incubations. In June, few changes were observed over the course of the incubations, mainly a slight but consistent decrease in abundance of several *Alphaproteobacteria* and *Bacteroidota* clades. Changes in community in September were diverse and did not follow an overall trend, except that in chondroitin sulfate incubations, *Flavicella* notably increased in abundance after 72 h. In February, while *Actinobacteriota* (mainly *Candidatus* Actinomarina) declined in proportion, members of the SAR11 clade and the gammaproteobacterial clade SAR86 were clearly overgrown by *Gammaproteobacteria* (mainly *Colwellia* and *Thalassotalea*) from 72 h on. Since in the unamended control many of the clades also changed in abundance in similar proportions, these changes cannot be attributed directly to polysaccharide utilization; such changes are known as 'bottle effects'. These changes are observable for the clades 'Marine Methylotrophic Group 3' and *Colwellia* in April, and also apply to a range of other genera. The strongest substrate-dependent response was found for members of the bacteroidotal *Flavicella*. They increased in the late phase of the chondroitin sulfate incubations in May and February, as well

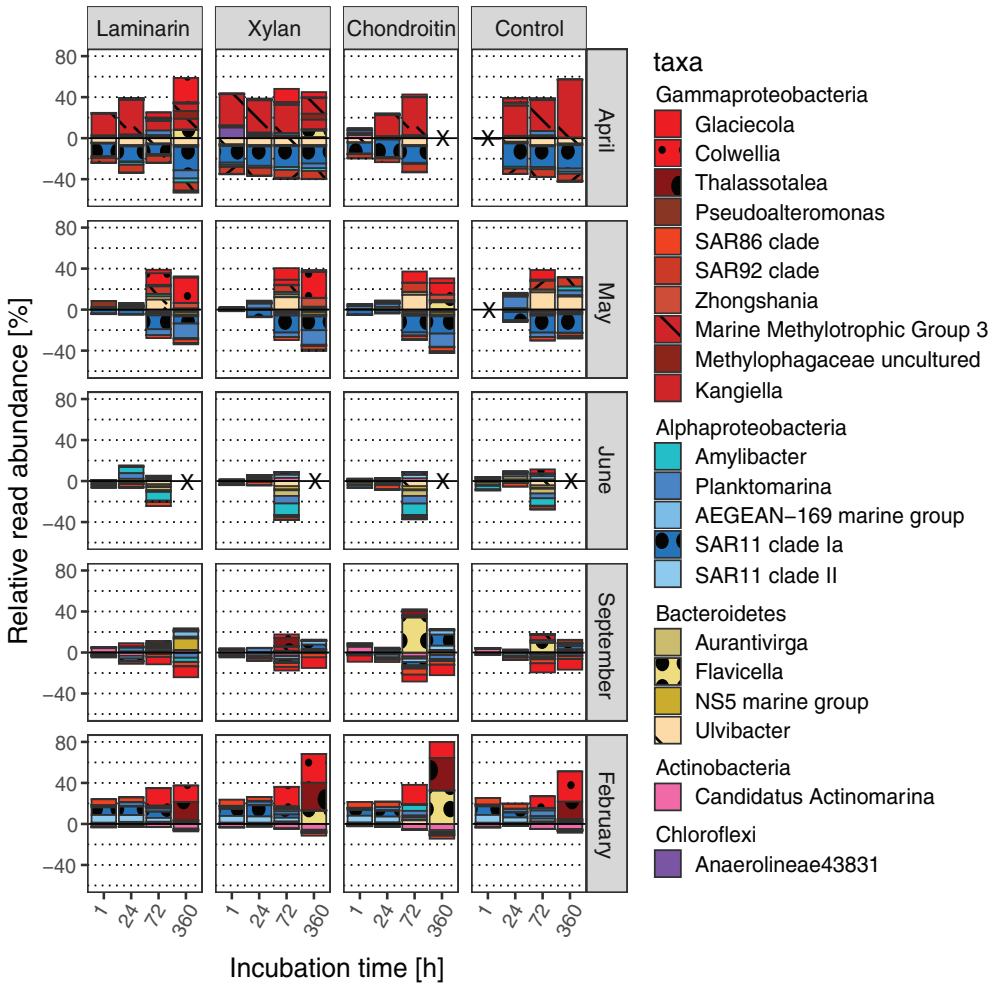

Fig. 3. Shift in the bacterial community in FLA-PS incubations and the unamended treatment control during all sampling times. Bars represent the shift in 16S rRNA sequence abundance of individual taxa relative to the initial community and average up to six replicates. Note that the initial community in May could not be sequenced and therefore the community after 1 h of the control was used instead. Taxa with a change of more than 5% are depicted. Time points marked with an x were not analysed.

as in the xylan incubation in February, a pattern not seen in the unamended control. In addition, they showed a strong but short-term increase in abundance at 72 h in the chondroitin and the unamended control incubations in September. Additionally, the alphaproteobacterial SAR11 and AEGEAN-169 marine group peaked in abundance at 360 h in the autumn chondroitin incubation.

Verrucomicrobiota *and* Planctomycetota *contribute to rapid selfish laminarin uptake in June*

Selfish uptake among members of the bacterial community was highest in June (Fig. 1C). Although 60% of all cells were fluorescently stained by FLA-laminarin within 24 h, tag sequencing provided no indication of a substrate-dependent increase of a particular bacterial clade (Fig. 3; Supplementary Figs S7–S8). In an effort to identify potentially selfish bacteria, we flow cytometrically tracked the rise of two broad and one narrow populations within the first 24 h of incubation (Fig. 4A–C) using a green fluorescence over side scatter dotplot diagram.

Two broad clusters, potentially corresponding to FLA-laminarin stained cells, were identified by comparison with an unstained negative control (Supplementary Fig. S12). Cells falling into the clusters with low (low FLA-lam) and medium (medium FLA-Lam) signal intensities (Fig. 4C) were flow cytometrically sorted. Microscopic examination of both clusters showed that the sorts did not represent pure populations of substrate-stained cells, but were mixtures of only a few FLA-laminarin stained cells and fluorescent debris originating most likely from free FLA-laminarin attached to dispersed organic matter (Fig. 4D and E). In the medium FLA-lam population, only

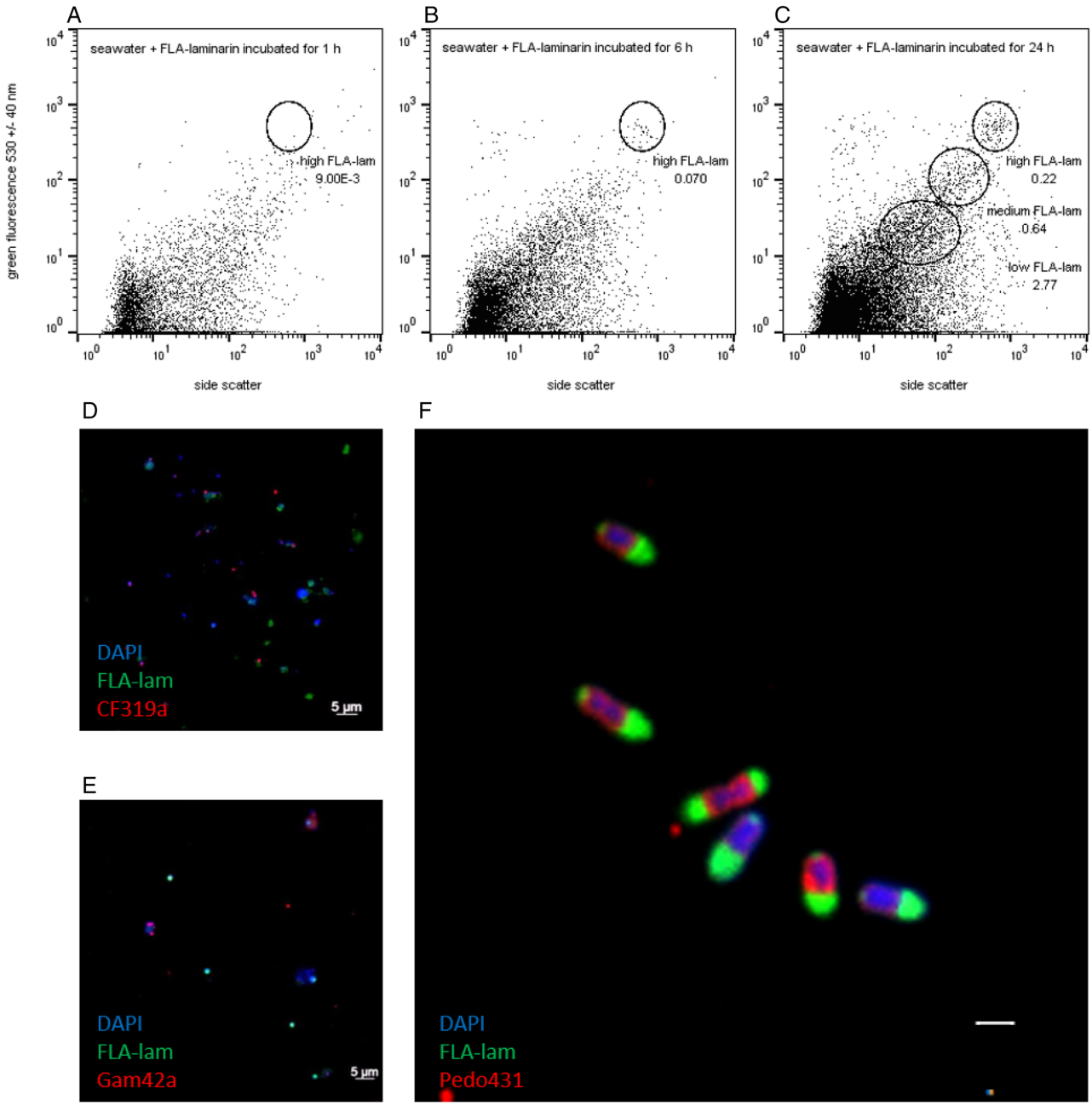

Fig. 4. FLA-laminarin stained population developing over 24 h of incubation in June. Flow cytometric scatter plot shows the development of FLA-laminarin stained cells from (A) 1 h over (B) 6 h to (C) 24 h. Each plot depicts 10 000 events. The three populations representing cell stained at low, medium and high intensity with FLA-laminarin were enriched via fluorescence-activated cell sorting (FACS). Numbers below the gate labels indicate the percentage of total events falling into this gate. Microscopic analysis showed the staining intensity and pattern of the cells from the (D) low, (E) medium and (F) highly FLA-laminarin (FLA-lam) stained populations. Scale bar in F = 1 µm.

about 23% of sorted cells were selfish laminarin utilizers. We hybridized sorted cells of this population with probes specific for the abundant *Bacteroidota*, *Gamma-* and *Alphaproteobacteria* from sequencing analysis, and also with probes for the less represented *Verrucomicrobiota* and *Planctomycetota*, as members of these phyla are also known to stain with FLA-PS (Martinez-Garcia *et al*., 2012; Reintjes *et al*., 2017, Reintjes *et al*., 2019; Boedeker *et al*., 2017). Most of these FLA-laminarin stained cells (82%) were in fact single coccoid *Planctomycetota* cells with a characteristic monopolar FLA-PS accumulation pattern.

From the distinct cluster with strong fluorescence we sorted a morphologically homogenous population of

elongated cells with a conspicuous bipolar FLA-laminarin accumulation pattern (Fig. 4F, Supplementary Fig. S13). These cells hybridized exclusively with the EUB388-III probe, specific for members of the *Verrucomicrobiota*. Fluorescence *in situ* hybridization (FISH) counts (Fig. 5A) and 16S tag sequences (Fig. 5B) suggested that these verrucomicrobia could be affiliated with *Rubritaleaceae*, *Opitutales* and *Pedosphaeraceae*. Therefore, we sorted high FLA-lam cells for 16S rRNA tag sequencing, and found that sequences from the *Pedosphaeraceae* far outnumbered those of the *Rubritaleaceae* and *Opitutales* in the sorted fraction (Fig. 5C). This finding was confirmed by FISH: virtually all cells from the high FLA-lam hybridized with the Pedo431 probe and therefore were affiliated with the *Pedosphaeraceae* (Fig. 4F, Supplementary Fig. S13). However, even though they are obviously efficient in selfish FLA-laminarin uptake, members of these *Pedosphaeraceae* did not increase in either relative (Fig. 5B, Supplementary Figs S7–S8) or in absolute abundance (Fig. 5A) within the initial 24 h of the incubations.

Discussion

Shifting contributions of extracellular hydrolysis and selfish uptake over a seasonal cycle

Bacterial communities in our incubations from five different sampling time points fall into three significantly different clusters (Fig. 2A), each cluster characterized by the ability to utilize polysaccharides at a different speed and through different modes. These differences in initial bacterial communities, with their distinct enzymatic repertoires, most likely explain differences in modes of bacterial polysaccharide processing. Within a cluster, differences in speed of response – between April and May communities, for example – are likely due to substrate-induced expression of genes for polysaccharide utilization, leading to polysaccharide utilization at earlier timepoints during the incubation (Reintjes *et al*., 2017; Reintjes *et al*., 2019).

Early onset of polysaccharide utilization – especially via selfish uptake – in our incubations was even more striking in the early and late summer samples from June and September, which also formed a cluster (Figs 1C and D and 2; Supplementary Figs S1–S3C–F). In addition to effects that might be due to the higher temperatures and therefore higher enzymatic turnover, community effects were evident, in particular a second bacterial cluster of fast polysaccharide degraders that took over the community (Fig. 2A, Supplementary Figs S7–S10). In addition to the rapid onset of substrate processing, these communities showed high extracellular hydrolysis rates (especially of chondroitin and xylan in September), and a high percentage of selfish cells. The mode and type of polysaccharide utilized, however, shifted from mainly laminarin and xylan selfish uptake in June to external hydrolysis of chondroitin sulfate and xylan in September. This shift accompanied a reduction in relative abundance of *Bacteroidota* and *Verrucomicrobiota* as well as an increase in *Gammaproteobacteria* and *Actinobacteria* at these time points. Given that members within these taxonomic groups are reported to have the capability for polysaccharide utilization (Garcia *et al*., 2013; Cardman *et al*., 2014; Sarmento *et al*., 2016; Reintjes *et al*., 2017; Sichert *et al*., 2020), our observations suggest that they readily express the enzymatic machinery for fast polysaccharide utilization in June and September, but occupy different ecological niches. This fine-tuned specialization allows them to thrive on different polysaccharides as

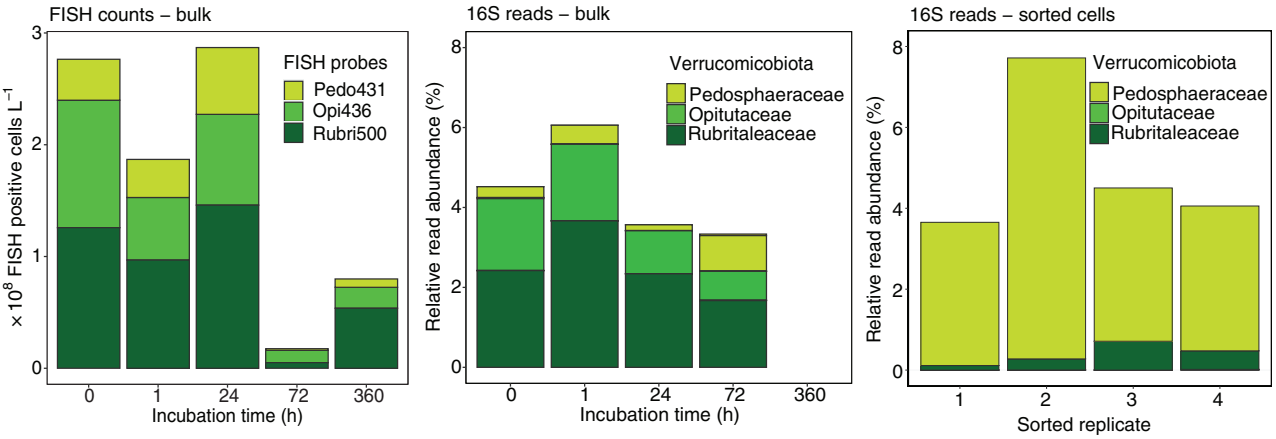

Fig. 5. Verrucomicrobiotal taxa in FLA-laminarin incubations in summer.
A. Average absolute abundance of selected verrucomicrobiotal clades of the bulk community from triplicate incubations.
B. Relative 16S rRNA sequence abundance of verrucomicrobiotal clades from the bulk community.
C. Relative 16S rRNA sequence abundance of verrucomicrobiotal clades from the high-lam sorted population after 24 h of incubation.

substrates, making preferential use of either selfish uptake or extracellular hydrolysis.

One niche-determining factor is a bacterium's energetic investment to acquire and process polysaccharides. Energy invested in the expression of a large set of carbohydrate-active enzymes needs to be balanced by the uptake of hydrolysis products. In the case of external hydrolysis, some of these products are lost to the surrounding environment in dilute environments such as the water column (Drescher *et al*., 2014; Traving *et al*., 2015). Bacteria associated with or attached to particles and aggregates can minimize the energetic loss, as the surrounding substrate density is high (Grossart *et al*., 2003; Traving *et al*., 2015), and they can share available substrates in their microhabitats (Corno *et al*., 2013). Considering high rates of extracellular chondroitin and xylan hydrolysis (Fig. 1D) together with high abundance of *Gammaproteobacteria* and *Actinobacteria* (Fig. 3, Supplementary Figs S9 and S10) that are known to colonize marine aggregates (Grossart *et al*., 2004), we speculate that particle-associated bacteria in September contributed considerably to polysaccharide utilization via external hydrolysis. Microscopic analysis showing a high abundance of large particles with attached microorganisms (Supplementary Fig. S14) supports this hypothesis.

While the summer community seemed to thrive on readily available polysaccharides, we observe a third separate NMDS cluster of the February community (Fig. 2A). This community, sampled in a typical winter situation with low temperatures and after months of low phytoplankton abundance, showed low polysaccharide utilization activity, with low selfish uptake of substrates other than laminarin, and external hydrolysis measurable only upon extended incubation (Fig. 1C and D). The resident bacterial community likely has a small fraction of organisms ready to respond to polysaccharide input at this time. These prominent differences in the mode, speed and type of polysaccharide utilization suggest that over the seasons, the bacterial communities in coastal surface waters differ greatly in their ability to utilize marine polysaccharides, with the most rapid responses to changing polysaccharide inputs occurring between May and September.

Many different bacteria perform rapid selfish polysaccharide uptake

The highest relative abundance of selfish bacteria was found in the midst of a centric diatom bloom in June (Fig. 1A and C). At this time, 60% of the community took up laminarin, the highest percentages ever reported for selfish laminarin uptake in surface ocean waters (25% in Reintjes *et al*., 2017; 32% in Reintjes *et al*., 2019; 28% in Reintjes *et al*., 2020a; 45% in Reintjes *et al*., 2020b). Furthermore, the speed at which intracellular substrate accumulation was detectible in the incubation – within few hours – is indicative of prior substrate induction (e.g. Reintjes *et al*., 2017). The resident bacterial community was clearly prepared for a fast selfish laminarin uptake, suggesting that laminarin was readily available for uptake for some time before the date of sampling.

Our data strongly suggest that the ability to take up laminarin selfishly must be widespread among bacteria, since more than half of the diverse community mainly composed of *Gamma-* and *Alphaproteobacteria*, *Bacteroidota*, *Actinobacteria* and *Verrucomicrobiota* showed selfish uptake within hours (Fig. 1, Supplementary Figs S7 and S8). Moreover, despite strong changes in total cell numbers, the community composition stayed comparatively constant over the course of the incubation, with only a slight increase in *Actinobacteria* and a wider range of low-abundance bacterial groups, late in the incubation. One part of the laminarin utilization was doubtlessly carried out by members of the *Bacteroidota*, confirming prior observations in spring blooms (e.g. Teeling *et al*., 2016; Kappelmann *et al*., 2019; Krüger *et al*., 2019). They reach maximal annual abundance in June. Members of the *Flavobacteriaceae* were described previously to harbour multiple polysaccharide utilization loci that are induced once the respective substrate is available (Unfried *et al*., 2018; Francis *et al*., 2021). Based on correlation of cell numbers and selfish uptake, we particularly suspect *Ca*. Prosiliicoccus and *Aurantivirga* to contribute to laminarin uptake, since they together account for 15% of the June community. However, the contribution to laminarin uptake of other taxa beyond the *Bacteroidota* could not be pinpointed solely by correlation between NGS sequencing and selfish uptake. In addition, we therefore also directly linked laminarin uptake to the identification of bacterial taxa through flow cytometric sorting.

Selfish Verrucomicrobiota *identified through flow cytometric sorting of intensely FLA-laminarin stained cells*

Microscopic analyses demonstrated diverse patterns of cellular polysaccharide accumulation, including a characteristic strong bipolar staining of a rather rare large cell type (Supplementary Fig. S15). This observation supports the idea that a wide range of bacteria must have selfishly taken up laminarin in June. These laminarin utilizers exhibited a broad range of fluorescence intensities, from cells with low intensity due to diffuse substrate distributions across the entire cell interior to cells with striking substrate signals accumulated at the cell poles. We flow cytometrically sorted these cells, allowing us to identify them as *Pedosphaeraceae* of the

phylum *Verrucomicrobiota*. These cells are selfish laminarin uptake specialists, showing rapid substrate utilization in June (Fig. 4A–C, F, Supplementary Fig. S13).

Although the *Pedosphaeraceae* themselves only account for a few percent (3% relative abundance; Supplementary Figs S7 and S8) of the total bacterial community, their intense substrate staining implies that they contribute disproportionately to the total laminarin turnover. Accumulation of such high amounts of FLA-laminarin at the cell poles within just 24 h of incubation suggests that members of the *Pedosphaeraceae* must run an effective polysaccharide uptake machinery, despite the fact that they do not possess the Sus-like high-affinity transport system well-studied in *Bacteroidota* (Cho and Salyers, 2001; Koropatkin *et al*., 2012). They do, however, have a multitude of glycoside hydrolases and TonB-dependent receptors for active transport through the outer membrane (Martinez-Garcia *et al*., 2012; Orellana *et al*., 2021). The precise means by which they rapidly take up laminarin into their periplasm needs to be explored in future studies.

Selfish uptake of polysaccharides thus appears to be widespread among members of bacterial communities. Although this mechanism of substrate utilization was initially identified among gut-associated members of the *Bacteroidota* (Cuskin *et al*., 2015), other bacterial clades – including numerically minor members of communities – use it to their advantage in aquatic systems. The contributions of these diverse organisms, whose abundances and activities vary throughout the year, are an important but previously overlooked aspect of heterotrophic carbon cycling. Given that selfish uptake reduces the production and availability of low-molecular-weight hydrolysis products in the environment, selfish bacteria likely have a structuring effect on the entire microbial community.

In summary, our study revealed a pronounced seasonality of polysaccharide utilization throughout the year. It is highest in summer and early fall, as a response to enhanced primary production, which triggers a rapid response to this type of fixed carbon. Most notably, our results demonstrate that polysaccharide utilization – including selfish uptake – is more widely spread among microbial clades than would be anticipated from bioinformatic predictions, an observation that highlights the importance of hypothesis testing in the environment. In addition to the well-known bacteroidotal players whose polysaccharide processing capabilities are well established (e.g. Reintjes *et al*., 2017), other still-to-be identified polysaccharide consumers play an important role. This point is well-illustrated by the highly efficient selfish *Pedosphaeraceae*, which we were able to identify in this study. Doubtless more species that play key roles in driving the cycling of complex polysaccharides – and thus a considerable fraction of marine primary productivity – are waiting to be discovered.

Experimental procedures

Sampling and substrate incubation

Surface seawater samples were collected in April, May, June and September 2018 and February 2019 at Helgoland Roads in the North Sea (see Supplementary experimental procedures S1 for details). Triplicate seawater samples were incubated at *in situ* temperature for up to 360 h with fluorescently labelled laminarin, xylan, or chondroitin sulfate (3.5 μM monomer equivalent) along with an unamended treatment control and an autoclaved killed control. Subsamples for cell counts, selfish FLA-PS uptake analysis, measurements of extracellular FLA-PS hydrolysis, FISH analysis and FACS were taken after 0, 1, 6, 12, 24, 48, 72, 96 and 360 h of incubation. Subsamples for bulk DNA analysis were taken at 0, 24, 72 and 360 h of incubation. Environmental data and phytoplankton abundances were recorded in parallel throughout the years 2018 and 2019 as part of the Helgoland Roads time series (Wiltshire *et al*., 2008; http://www.pangaea.de).

Taxonomic analysis

For taxonomic analysis of the initial bacterial communities and their changes over the course of the incubation, 10 ml sample from each incubation were filtered unfixed. Total DNA extraction from filter was done with the DNeasy Power Water Kit (Qiagen). The hypervariable V3/V4 region (490 bp) of the 16S rRNA was amplified (see Supplementary experimental procedures S1 for primer details), size selection and purification of the amplified PCR product was done using the AMPure XP PCR Cleanup system (Beckman Coulter). Barcoded products were pooled in equimolar concentrations for emulsion PCR with the Ion Torrent One-Touch System (Thermo Fischer Scientific) and sequenced on an IonTorrent PGM™ sequencer (Thermo Fischer Scientific) using the High-Q™ and High-Q View chemistry (Thermo Fischer Scientific). Demultiplexing and quality trimming was done using Mothur (Schloss *et al*., 2009). The SILVAngs pipeline (Quast *et al*., 2013) was used with the SSU rRNA SILVA database 138.1 (ref NR 99) for sequence comparison and taxonomic assignment of the retrieved sequences.

Flow cytometric measurements and sorting

Formaldehyde fixed cell samples from 1, 6 and 24 h of FLA-laminarin incubations in June were flow cytometrically

analysed using a BD Influx™ Cell Sorter (BD biosciences) with a 100 mW UV-laser (355 nm, Coherent) and a 200 mW Coherent Sapphire laser (488 nm, Coherent). Cell characteristics in the sideward angle light scatter (SSC), the cells' stained DNA and the green fluorescence FLA-PS signal were detected and recorded with the BD biosciences FACS™ Software version 1.2 (BD biosciences) and analysed with the FlowJo® v10 flow cytometry analysis software (BD biosciences). Three populations were selected from the 24 h incubation sample for sorting (Fig. 4C), representing events with high (high FLA-lam), medium (medium FLA-lam) and low (low FLA-lam) green fluorescence intensity (Supplementary Fig. S12). Cell sorting was performed in a twofold way at highest purity. Replicates of 1×10^4 cells were sorted based on DNA and FLA-laminarin signal, excluding autofluorescence. The taxonomic composition of cells from the high FLA-lam population was analysed by direct amplification of 16S rRNA. Cells from all sorted populations were filtered and subjected to FISH and subsequent microscopic analysis.

Oligonucleotide probe design and fluorescence in situ *hybridization*

Oligodeoxynucleotide probes with competitor probes were designed from bulk 16S sequences, covering the *Opitutales* (Opi346), *Pedosphaeraceae* (Pedo431) and *Rubritaleaceae* (Rubri500) (Supplementary Table S2). FISH with slight alterations of the protocol by Manz *et al*. (1992) was carried out for bacterial identification and quantification, using four times Atto-594 labelled oligo-probes (Supplementary Table S2) for bacteria in general (EUB388-I), *Gammaproteobacteria* (GAM42a), *Bacteroidota* (CF319a), *Planctomycetota* (PLA46), *Verruomicrobiota* (EUB338-III), *Rubritaleaceae* (Rubri500), *Pedosphearae* (Pedo431) and *Opitutales* (Opi346).

Cell enumeration and substrate staining

For the enumeration of total microbial cell numbers, FLA-PS stained cells and FISH, 20–30 ml of formaldehyde fixed sample were filtered. The DNA was counterstained with DAPI and cells were visualized after mounting using a fully automated epifluorescence microscope (Zeiss Axio Imager.Z2 microscope stand, Carl Zeiss) equipped with a cooled charged-coupled-device camera (AxioCam MRm + Colibri LED light source, Carl Zeiss), three light-emitting diodes (UV-emitting LED, for DAPI; blue-emitting LED for FLA-PS; yellow-emitting LED for FISH) and a HE-62 multifilter module with a triple emission filter (Carl Zeiss). A minimum of 45 fields of view were acquired as described by Bennke *et al*. (2016) and cell counting was performed with the image analysis software ACMETOOL (Max Planck Institute for Marine Microbiology, Bremen; https://www.mpi-bremen.de/en/automated-microscopy.html). Manual cell counting was done to validate the automated counts.

Super-resolution microscopy

The FLA-PS uptake pattern was visualized on a Zeiss LSM 780 with Airyscan (Carl Zeiss). In the setup, 405, 488 and 561 nm lasers with respective detection windows of 420–480, 500–550 and LP 605 nm were used and images were taken with a Plan-Apochromat 63×/1.4 Oil objective in Z-stack mode. Airyscan processing was done using the ZEN software package (Carl Zeiss).

Measurement of extracellular enzymatic activity

The polysaccharides laminarin, xylan and chondroitin sulfate (Sigma Aldrich) were fluorescently labelled with fluoresceinamine (Sigma Aldrich; isomer II) as described by Arnosti (2003). To measure extracellular enzymatic hydrolysis, water from the FLA-laminarin, FLA-xylan and FLA-chondroitin and the respective killed controls was filtered through a 0.2 μm polycarbonate filter. The filtrate was analysed using gel permeation chromatography with fluorescence detection to track the change in molecular weight from the initial polysaccharide to lower molecular weight hydrolysis products (Arnosti, 1996; Arnosti, 2003). Chromatograms were checked manually. Hydrolysis rates were calculated as described in detail in Arnosti (2003).

Statistical analysis

Community composition analysis was done on normalized samples representing >10 000 sequences. Archaeal and eukaryal reads were excluded and the average of 1–6 replicates was used for further analysis and visualization. Differences in the community composition between seasons, incubation times, and substrate amended to unamended incubations were analysed by analysis of similarity (ANOSIM) and visualized in NMDS plots, using Bray–Curtis dissimilarity matrices. The influence of measured environmental conditions on the NMDS ordinations was calculated by the correlation between dissimilarity indices and the gradient separation. A visual representation of the community shift over the course of the incubation was done by the comparison of the genus-specific sequence abundance from the initial community to the respective sequence abundance over time.

Data availability

The Ion Torrent-generated libraries of bacterial 16S rRNA gene sequences were archived at the European Nucleotide Archive (ENA) of The European Bioinformatics Institute (EMBL-EBI) under the accession number PRJEB35938. Flow Cytometry datasets are archived at the FlowRepository database under the accession number FR-FCM-Z365.

Acknowledgements

We thank Antje Wichels, Eva-Maria Brodte and Uwe Nettelmann from the Biologische Anstalt Helgoland for enabling and facilitating the sample collection and incubation experiments on Helgoland. Furthermore, we would like to thank the crew of the *Aade* for water sample collection, Karen H. Wiltshire and the Helgoland Roads team for support and analysis of the physicochemical parameters and phytoplankton counts. We are also grateful to Nevena Maslac, Taylor Priest for help with sequencing work, Maria Belén Gonzalez Pino for help with sample collection and microscopy, Andreas Ellrott for help with microscopy techniques, Jan Brüwer for help with the Airyscan imaging and taking the STED images, Zarah Janda for help with microscopy and FISH analysis, and Sherif Ghobrial for help with measurements of polysaccharide hydrolase activities. This study was supported by the Max Planck Society and the German Research Foundation (DFG) project FOR 2406 Proteogenomics of Marine Polysaccharide Utilization (POMPU) by grants of Bernhard Fuchs (FU 627/2-1), as well as funding by the U.S. National Science Foundation to CA (OCE-1736772 and OCE-2022952).

References

Aluwihare, L.I., and Repeta, D.J. (1999) A comparison of the chemical characteristics of oceanic DOM and extracellular DOM produced by marine algae. *Mar Ecol Prog Ser* **186**: 105–117.

Arnosti, C. (1995) Measurement of depth- and site-related differences in polysaccharide hydrolysis rates in marine sediments. *Geochim Cosmochim Acta* **59**: 4247–4257.

Arnosti, C. (1996) A new method for measuring polysaccharide hydrolysis rates in marine environments. *Org Geochem* **25**: 105–115.

Arnosti, C. (2003) Fluorescent derivatization of polysaccharides and carbohydrate-containing biopolymers for measurement of enzyme activities in complex media. *J Chromat B* **793**: 181–191.

Arnosti, C. (2008) Functional differences between Arctic seawater and sedimentary microbial communities: contrasts in microbial hydrolysis of complex substrates. *FEMS Microbiol Ecol* **66**: 343–351.

Arnosti, C., and Jørgensen, B.B. (2006) Organic carbon degradation in arctic marine sediments, Svalbard: a comparison of initial and terminal steps. *Geomicrobiol J* **23**: 551–563.

Arnosti, C., Reintjes, G., and Amann, R. (2018) A mechanistic microbial underpinning for the size-reactivity continuum of dissolved organic carbon degradation. *Mar Chem* **206**: 93–99.

Arnosti, C., Steen, A.D., Ziervogel, K., Ghobrial, S., and Jeffrey, W.H. (2011) Latitudinal gradients in degradation of marine dissolved organic carbon. *PLoS One* **6**: 1–6.

Arnosti, C., Wietz, M., Brinkhoff, T., Probandt, D., Zeugner, L., and Amann, R. (2021) The biogeochemistry of marine polysaccharides: sources, inventories, and bacterial drivers of the carbohydrate cycle. *Ann Rev Mar Sci* **13**: 81–108.

Azam, F., Fenchel, T., Field, J.G., Gray, J.S., Meyer-Reil, L. A., and Thingstad, F. (1983) The ecological role of water-column microbes in the sea. *Mar Ecol Prog Ser* **10**: 257–263.

Balmonte, J.P., Teske, A., and Arnosti, C. (2018) Structure and function of high Arctic pelagic, particle- associated and benthic bacterial communities. *Environ Microbiol* **20**: 2941–2954.

Bennke, C.M., Reintjes, G., Schattenhofer, M., Ellrott, A., Wulf, J., Zeder, M., and Fuchs, B.M. (2016) Modification of a high-throughput automatic microbial cell enumeration system for shipboard analyses. *Auto Microb Cell* **82**: 3289–3296.

Biersmith, A., and Benner, R. (1998) Carbohydrates in phytoplankton and freshly produced dissolved organic matter. *Mar Chem* **63**: 131–144.

Boedeker, C., Schüler, M., Reintjes, G., Jeske, O., van Teeseling, M.C.F., Jogler, M., *et al*. (2017) Determining the bacterial cell biology of *Planctomycetes*. *Nat Commun* **8**: 1–14.

Cardman, Z., Arnosti, C., Durbin, A., Ziervogel, K., Cox, C., Steen, A.D., and Teske, A. (2014) *Verrucomicrobia* are candidates for polysaccharide-degrading bacterioplankton in an arctic fjord of Svalbard. *Appl Environ Microbiol* **80**: 3749–3756.

Cho, K.H., and Salyers, A.A. (2001) Biochemical analysis of interactions of outer membrane proteins that contribute to starch utilization by *Bacteroidetes thetaiotaomicon*. *J Bacteriol* **183**: 7224–7230.

Corno, G., Villiger, J., and Pernthaler, J. (2013) Coaggregation in a microbial predator – prey system affects competition and trophic transfer efficiency. *Ecology* **94**: 870–881.

Cuskin, F., Lowe, E.C., Temple, M.J., Zhu, Y., Cameron, E. A., Pudlo, N.A., *et al*. (2015) Human gut *Bacteroidetes* can utilize yeast mannan through a selfish mechanism. *Nature* **517**: 165–169.

Drescher, K., Nadell, C.D., Stone, H.A., Wingreen, N.S., and Bassler, B.L. (2014) Solutions to the public goods dilemma in bacterial biofilms. *Curr Biol* **24**: 50–55.

Dunny, G.M., Brickman, T.J., and Dworkin, M. (2008) Multicellular behavior in bacteria: communication, cooperation, competition and cheating. *BioEssays* **30**: 296–298.

Francis, T.B., Bartoski, D., Sura, T., Sichert, A., Hehemann, J.-H., Markert, S., *et al*. (2021) Changing expression patterns of TonB-dependent transporters suggest shifts in polysaccharide consumption over the course of a spring phytoplankton bloom. *ISME J* **15**: 2336–2350.

Francis, T.B., Krüger, K., Fuchs, B.M., Teeling, H., and Amann, R. (2019) *Candidatus* Prosiliicoccus vernus, a spring phytoplankton bloom associated member of the *Flavobacteriaceae*. *Syst Appl Microbiol* **42**: 41–53.

Garcia, S.L., McMahon, K.D., Martinez-Garcia, M., Srivastava, A., Sczyrba, A., *et al*. (2013) Metabolic potential of a single cell belonging to one of the most abundant lineages in freshwater bacterioplankton. *ISME J* **7**: 137–147.

Giljan, G., Brown, S., Lloyd, C.C., Ghobrial, S., Amann, R., and Arnosti, C. (2021) Selfish bacteria are active throughout the water column of the ocean. *bioRxiv*. https://doi.org/10.1101/2021.07.26.453833.

Grossart, H., Kiørboe, T., Tang, K., and Ploug, H. (2003) Bacterial colonization of particles: growth and interactions. *Appl Environ Microbiol* **69**: 3500–3509.

Grossart, H.P., Schlingloff, A., Bernhard, M., Simon, M., and Brinkhoff, T. (2004) Antagonistic activity of bacteria isolated from organic aggregates of the German Wassen Sea. *FEMS Microbiol Ecol* **47**: 387–396.

Helbert, W. (2017) Marine polysaccharide sulfatases. *Front Mar Sci* **4**: 1–10.

Hoarfrost, A., Balmonte, J.P., Ghobrial, S., Ziervogel, K., Bane, J., *et al*. (2019) Gulf stream ring intrusion on the mid-Atlantic bight shelf affects microbially-driven carbon cycling. *Front Mar Sci* **6**: 1–13.

Kappelmann, L., Krüger, K., Hehemann, J.-H., Harder, J., Markert, S., Unfried, F., *et al*. (2019) Polysaccharide utilization loci of North Sea *Flavobacteriia* as basis for using SusC/D-protein expression for predicting major phytoplankton glycans. *ISME J.* **13**: 76–91.

Koropatkin, N.M., Cameron, A.E., and Martens, E.C. (2012) How glycan metabolism shapes the human gut microbiota. *Nat Rev Microbiol* **10**: 323–335.

Krüger, K., Chafee, M., Francis, T.B., Glavina del Rio, T., Becher, D., Schweder, T., *et al*. (2019) In marine *Bacteroidetes* the bulk of glycan degradation during algae blooms is mediated by few clades using a restricted set of genes. *ISME J* **13**: 2800–2816.

Laine, R.A. (1994) Invited commentary: a calculation of all possible oligosaccharide isomers both branched and linear yields 1.05 x 10^{12} structures for a reducing hexasaccharide: The *Isomer Barrier* to development of sinle-method saccharide sequencing or synthesis systems. *Glycobiology* **4**: 759–767.

Lee, C., Wakeham, S., and Arnosti, C. (2004) Particulate organic matter in the sea: the composition conundrum. *Ambio* **33**: 565–575.

Manz, W., Amann, R., Ludwig, W., and Wagner, M. (1992) Phylogenetic oligodeoxynucleotide probes for the major subclasses of *Proteobacteria*: problems and solutions. *Syst Appl Microbiol* **15**: 593–600.

Martinez-Garcia, M., Brazel, D.M., Swan, B.K., Arnosti, C., Chain, p.S.G., Reitenga, K.G., *et al*. (2012) Capturing single cell genomes of active polysaccharide degraders: an unexpected contribution of *Verrucomicrobia*. *PLoS ONE* **7**: 1–11.

McCarthy, M., Hedges, J., and Benner, R. (1996) Major biochemical composition of dissolved higher molecular weight organic matter in seawater. *Mar Chem* **55**: 281–297.

Moran, M.A., Kujawinski, E.B., Stubbins, A., Fatland, R., Aluwihare, L.I., Buchan, A., *et al*. (2016) Deciphering Ocean carbon in a changing world. *Proc Natl Acad Sci U S A* **113**: 3143–3151.

Orellana, H.L., Francis, T.B., Ferraro, M., Hehemann, J.-H., Fuchs, B.M., and Amann, R.I. (2021) Verrucomicrobiota are specialized consumers of sulfated methyl pentoses during diatom blooms. *ISME J* **38**: 1–12.

Quast, C., Pruesse, E., Yilmaz, P., Gerken, J., Schweer, T., Yarza, P., *et al*. (2013) The SILVA ribosomal RNA gene database project: improved data processing and web-based tools. *Nucl Acids Res* **41**: 590–596.

Reintjes, G., Arnosti, C., Fuchs, B., and Amann, R. (2019) Selfish, sharing and scavenging bacteria in the Atlantic Ocean: a biogeographical study of bacterial substrate utilization. *ISME J* **13**: 1119–1132.

Reintjes, G., Arnosti, C., Fuchs, B.M., and Amann, R. (2017) An alternative polysaccharide uptake mechanism of marine bacteria. *ISME J* **11**: 1640–1650.

Reintjes, G., Fuchs, B.M., Amann, R., and Arnosti, C. (2020b) Extensive microbial processing of polysaccharides in the South Pacific Gyre via selfish uptake and extracellular hydrolysis. *Front Microbiol* **11**: 1–14.

Reintjes, G., Fuchs, B.M., Scharfe, M., Wiltshire, K.H., Amann, R., and Arnosti, C. (2020a) Short-term changes in polysaccharide utilization mechanisms of marine bacterioplankton during a spring phytoplankton bloom. *Environ Microbiol* **22**: 1884–1900.

Sarmento, H., Morana, C., and Gasol, J.M. (2016) Bacteriplankton niche partitioning in the use of phytoplankton-derived dissolved organic carbon: quantity is more important than quality. *ISME J* **10**: 2582–2592.

Schloss, p.D., Westcott, S.L., Ryabin, R., Hall, J.R., Hartmann, M., Hollister, E.B., *et al*. (2009) Introducing mothur: open-source, platform-independent, community-supported software for describing and comparing microbial communities. *Appl Environ Microbiol* **75**: 7537–7541.

Sichert, A., Corzett, C.H., Schechter, M.S., Unfried, F., Markert, S., Becher, D., *et al*. (2020) *Verrucomicrobia* use hundreds of enzymes to digest the algal polysaccharide fucoidan. *Nat Microbiol* **5**: 1–14.

Teeling, H., Fuchs, B.M., Becher, D., Klockow, C., Gardebrecht, A., Bennke, C.M., *et al*. (2012) Substrate-controlled succession of marine bacterioplankton populations induced by a phytoplankton bloom. *Science* **336**: 608–611.

Teeling, H., Fuchs, B.M., Bennke, C.M., Krüger, K., Chafee, M., Kappelmann, L., *et al*. (2016) Recurring patterns in bacterioplankton dynamics during coastal spring algae blooms. *eLife* **5**: e11888.

Traving, S.J., Thygesen, U.H., Riemann, L., and Stedmon, A. (2015) A model of extracellular enzymes in free- living microbes: which strategy pays off? *Appl Environ Microbiol* **81**: 7385–7393.

Unfried, F., Becker, S., Robb, C. S., Hehemann, J.-H., Markert, S., Heiden, S. E. et al. (2018) Adaptive mechanisms that provide competitive advantages to marine bacteroidetes during microalgal blooms. *ISME J.* **12**: 2894-2906.

Wiltshire, K.H., Malzahn, A.M., Wirtz, K., Greve, W., Janisch, S., Mangelsdorf, P., *et al*. (2008) Resilience of North Sea phytoplankton spring bloom dynamics: an analysis of long-term data at Helgoland Roads. *Limnol Oceanogr* **53**: 1294–1302.

Supporting Information

Additional Supporting Information may be found in the online version of this article at the publisher's web-site:

Supplementary Fig. S1. Total cell counts from the (A) first and (B) second sampling time point per sampling week, relative abundance of FLA-laminarin stained cells from the (C) first and (D) second sampling time point per sampling week, and extracellular polysaccharide hydrolysis rates from the (E) first and (F) second sampling time point per sampling week in FLA-laminarin amended incubations in each season. Error bars indicate the standard deviation from six replicates. The black line in (A) and (B) represents averaged total bacterial counts from the unamended treatment control. Time points marked with an x were not sampled.

Supplementary Fig. S2. Total cell counts from the (A) first and (B) second sampling time point per sampling week, relative abundance of FLA-xylan stained cells from the (C) first and (D) second sampling time point per sampling week, and extracellular polysaccharide hydrolysis rates from the (E) first and (F) second sampling time point per sampling week in FLA-xylan amended incubations in each season. Error bars indicate the standard deviation from six replicates. The black line in (A) and (B) represents averaged total bacterial counts from the unamended treatment control. Time points marked with an x were not sampled.

Supplementary Fig. S3. Total cell counts from the (A) first and (B) second sampling time point per sampling week, relative abundance of FLA-chondroitin stained cells from the (C) first and (D) second sampling time point per sampling week, and extracellular polysaccharide hydrolysis rates from the (E) first and (F) second sampling time point per sampling week in FLA-chondroitin amended incubations in each season. Error bars indicate the standard deviation from six replicates. The black line in (A) and (B) represents averaged total bacterial counts from the unamended treatment control. Time points marked with an x were not sampled.

Supplementary Fig. S4. Bacterioplankton community off Helgoland on the first sampling data in April in FLA-laminarin, FLA-xylan and FLA-chondroitin sulphate amended incubations in comparison to an unamended control. The first bar (0 h) represents the initial community. Bars represent the average of up to 6 replicates. Communities marked with an x were not analysed.

Supplementary Fig. S5. Bacterioplankton community off Helgoland on the second sampling data in April in FLA-laminarin, FLA-xylan and FLA-chondroitin sulphate amended incubations in comparison to an unamended control. The first bar (0 h) represents the initial community. Bars represent the average of up to 6 replicates. Communities marked with an x were not analysed.

Supplementary Fig. S6. Bacterioplankton community off Helgoland in May in FLA-laminarin, FLA-xylan and FLA-chondroitin sulphate amended incubations in comparison to an unamended control. The first bar should represent the initial community. Sequencing the initial community did not result in >10,000 sequences. Therefore, the community composition from the unamended incubation after just 1 h of incubation was chosen to be most representative for the initial community. Bars represent the average of up to 6 replicates.

Supplementary Fig. S7. Bacterioplankton community off Helgoland on the first sampling data in June in FLA-laminarin, FLA-xylan and FLA-chondroitin sulphate amended incubations in comparison to an unamended control. The first bar (0 h) represents the initial community. Bars represent the average of up to 6 replicates. Communities marked with an x were not analysed.

Supplementary Fig. S8. Bacterioplankton community off Helgoland on the second sampling data in June in FLA-laminarin, FLA-xylan and FLA-chondroitin sulphate amended incubations in comparison to an unamended control. The first bar (0 h) represents the initial community. Bars represent the average of up to 6 replicates. Communities marked with an x were not analysed.

Supplementary Fig. S9. Bacterioplankton community off Helgoland on the first sampling data in September in FLA-laminarin, FLA-xylan and FLA-chondroitin sulphate amended incubations in comparison to an unamended control. The first bar (0 h) represents the initial community. Bars represent the average of up to 6 replicates. Communities marked with an x were not analysed.

Supplementary Fig. S10. Bacterioplankton community off Helgoland on the second sampling data in September in FLA-laminarin, FLA-xylan and FLA-chondroitin sulphate amended incubations in comparison to an unamended control. The first bar (0 h) represents the initial community. Bars represent the average of up to 6 replicates. Communities marked with an x were not analysed.

Supplementary Fig. S11. Bacterioplankton community off Helgoland on the first sampling data in February in FLA-laminarin, FLA-xylan and FLA-chondroitin sulphate amended incubations in comparison to an unamended control. The first bar (0 h) represents the initial community. Bars represent the average of up to 6 replicates. Communities marked with an x were not analysed.

Supplementary Fig. S12. Flow cytometric dot plots of (A) negative control without FLA-PS addition and (B) FLA-laminarin amended incubation in June after 24 h of incubation.

Supplementary Fig. S13. Super resolution images of sorted FLA-laminarin stained cells (A) STED images showing the FLA-laminarin accumulation pattern and the respective DAPI nucleic acid counterstain. (B) LSM-Airyscan images showing the FLA-laminarin accumulation pattern, the respective DAPI nucleic acid counterstain, ribosomal RNA stained with the 4 x Atto594 labelled *Pedo431* FISH probe and an overlay of all three labels. Error bar = 2 μm.

Supplementary Fig. S14. Microscopic analysis of the amount and size of particles in the incubations at t = 0 h from (A) April, (B) May, (C) June, (D) September and (E) February. Bacteria stained with DAPI are visualized in blue, particles can be seen in green.

Supplementary Fig. S15. Overview on the diversity of microbial FLA-laminarin accumulation pattern after 24 h of FLA-laminarin incubations from summer seawater off Helgoland. All images were taken at a constant exposure time for

comparability of fluorescence signal intensity. Scale bars = 2 μm.

Supplementary Table S1. Biological and chemical metadata. No phytoplankton counts were obtained in February 2019. Chlorophyll *a* data were obtained from 10th April 2018 for spring sampling, from 28th June 2018 for summer sampling, from 18th September 2018 for autumn sampling.

Supplementary Table S2. Fluorescence *in situ* hybridization probe overview.

Supplementary experimental procedures S1.